Journal of The Physical Society of Japan
Vol. 60, No. 7, July, 1991, pp. 2406–2414

Three-Dimensional Antiferromagnetic Order and Anisotropic Magnetic Properties in Bi_2CuO_4

Kazuyoshi YAMADA, Ken-ichi TAKADA, Syoichi HOSOYA,[†]
Yousuke WATANABE,[†] Yasuo ENDOH, Norihisa TOMONAGA, Takashi SUZUKI,
Toru ISHIGAKI,[††] Takashi KAMIYAMA,[††]
Hajime ASANO[††] and Fujio IZUMI[†††]

Department of Physics, Tohoku University, Sendai 980
[†]Institute for Materials Research, Tohoku University, Sendai 980
[††]Institute of Materials Science, University of Tsukuba, Tsukuba 305
[†††]National Institute for Research in Inorganic Materials, Tsukuba 305

(Received March 13, 1991)

The structure and magnetic properties of Bi_2CuO_4 have been studied by neutron and X-ray diffraction, magnetic susceptibility and magnetization measurements. Three-dimensional (3D) and anisotropic antiferromagnetism is revealed for this compound rather than the previously anticipated one-dimensional one. Long-range antiferromagnetic order associated with a ferromagnetic stacking of Cu^{2+} spins along the [001] axis starts to develop below $T_N=42$ K. A magnetic moment of 0.85 ± 0.05 μ_B/Cu which is larger than those of Cu^{2+} spins in the two-dimensional Heisenberg antiferromagnets such as La_2CuO_4 and $Sr_2CuCl_2O_2$ reflects the 3D character in Bi_2CuO_4. A non-linear magnetization curve under an inplane magnetic field is analyzed quantitatively by a continuous spin rotation in the (001) plane.

[neutron diffraction, antiferromagnetism, Bi_2CuO_4, copper oxide]

§1. Introduction

Many types of layered cuprates with a 2–1–4 chemical formula have been extensively studied after the discovery of high-T_c superconducting 2–1–4 oxides. Anomalously strong two-dimensional (2D) antiferromagnetic correlations between Cu^{2+} spins in these oxides have been one of the main subjects for the elucidation of the superconducting mechanism. Bi_2CuO_4 is an another type of copper oxide which contains Cu^{2+} ions coordinated by oxygen atoms. As shown in Fig. 1 no 2D CuO_2 sheets are there as in the high-T_c copper oxides. Study of this compound, therefore, is expected to provide invaluable insight on the role of the 2D CuO_2 sheets for the high-T_c copper oxides.

Nearest neighbor Cu^{2+} ions in this compound are located along the [001] direction with a distance much shorter than that of second nearest neighbors. Hence the Cu^{2+} ions are regarded as being in a chain state. In fact, magnetic susceptibility measurements done by polycrystalline sample observed a broad peak around 50 K which is similar to that in one-dimensional (1D) antiferromagnets.[1] It was then proposed that Bi_2CuO_4 was one of model materials of $S=1/2$ Heisenberg antiferromagnetic chains. However, recent neutron diffraction measurements on powder samples revealed three-dimensional (3D) antiferromagnetic order.[2,3] They observed two magnetic Bragg peaks below 40.5 K. Relative intensities of these peaks are consistent with an antiferromagnetic structure with ferromagnetic stacking along the [001] direction and antiferromagnetic alignment between the second nearest neighbor spins. Furthermore, the moment of about 0.5 μ_B was evaluated by assuming a spin direction along the [001] direction.

As is described in the following sections, we have confirmed the 3D antiferromagnetizm in Bi_2CuO_4 by using single crystals. The present neutron diffraction study has proposed a new model for the spin structure. Furthermore, anisotropic magnetic properties such as

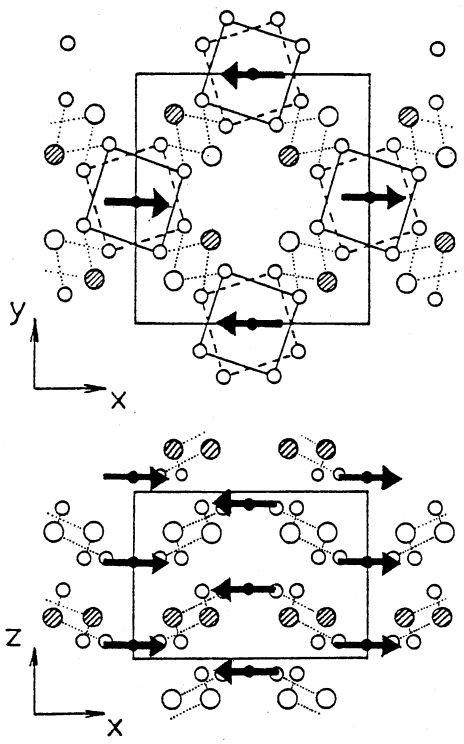

Fig. 1. Crystal structure of Bi_2CuO_4. Closed and open small circles are Cu and O atoms, respectively. Hatched or open larger circles are Bi atoms. Arrows in the figure indicate the orientation of the Cu^{2+} moment in the ordered state (§3.2). Dotted lines represent Bi–O bonds with the shortest length.

anisotropic g-values and a non-linear field dependence of the magnetization under the in-plane magnetic field have been presented and analyzed quantitatively.

§2. Experimental

Powder and small single crystals of Bi_2CuO_4 were prepared by solid-phase reaction. The mixture of Bi_2O_3 and CuO was heated in air for 72 h by raising the temperature slowly up to 800°C to avoid volatilization of Bi_2O_3. The product was ground and reheated at 830°C for 72 h. After the second reaction small single crystals of Bi_2CuO_4 were precipitated inside the polycrystalline sample. These crystals were used for X-ray diffraction measurements. The sample were reground into fine powder for a neutron powder diffraction measurement. Single crystal boules elongated along [001] with a typical dimension of 7 $mm^{\phi} \times 10$ mm were grown by a floating-zone method under controlled oxygen fugacity. Details of the growth will be described elsewhere.[4]

Before we started this study, two different space groups, i.e., P4/ncc and I4, had been proposed for the crystal structure of Bi_2CuO_4. Recent neutron powder[2,3] as well as Raman[5] measurements, however, confirmed the space group of P4/ncc proposed by Bovin *et al.*[6] rather than I4.[7] The reason for this difference in the results is probably due to the different temperature of synthesis of the specimens; Dissociation which occurs at higher temperatures was pointed out by Kakhan *et al.*[8] Therefore we examined the structure of our crystals by X-ray single-crystal and neutron powder diffraction measurements. X-ray measurements were performed at room temperature for the single crystal with a dimension of about $0.32 \times 0.22 \times 0.1$ mm^3 on a 4-circle diffractometer. The X-ray beam from CuK_{α} or MoK_{α} radiation was monochromatized by a pyrolytic graphite (PG) crystal. Second-order harmonics from the PG were reduced by a pulse height analyzer. Structural refinements could not be done because of huge attenuation of the X-ray beam in the crystal. Instead, extinction rules for both of the space groups, P4/ncc and I4, were checked. Furthermore several peaks which are observed in electron diffraction measurements[1] but not allowed for both of the space groups were reexamined carefully.

Neutron powder diffraction data were taken at room temperature on the HRP diffractometer installed at Booster Syncrotron Utilization Facility in KEK. The powder was contained in a cylindrical vanadium cell (10 $mm^{\phi} \times 42$ mm^{H} with 25 μm in thickness) in a vacuum chamber to reduce the background from air scattering. Neutrons scattered by the sample at around 170° were detected by ^3He proportional detectors. Time-of-flight (TOF) neutron data in a d-spacing (Q-spacing) range between 0.5 to 3.2 Å (12.4 to 1.9 $Å^{-1}$) were used for structure refinement. Overall Q-resolution is about 0.3% in this region.

Neutron diffraction measurements on the single crystals were carried out with the triple-axis neutron spectrometers of TUNS and TOPAN installed in the Japan Atomic Energy

Research Reactor JRR-2 and JRR-3, respectively. Incident neutron beam was monochromated into an energy of 13.7 or 30 meV, and higher-order reflected beam was filtered out by pyrolytic graphite crystals. The crystal was mounted in an Al container in which He gas was charged as a heat exchanger. By using a ^{4}He-closed type cryogenic system (CTI, Lake Shore), the temperature of the crystal was controlled with the resolution better than 0.5% between room temperature to 10 K.

The magnetic susceptibility and magnetization for both the powder and single crystals were measured by a vibrating-sample magnetometer between 3 K and 300 K with the external fields up to 2 T.

§3. Results and Discussion

3.1 Structure analysis

In preliminary X-ray single crystal measurements, three types of reflections were studied, i.e, (a) *hkl* reflections with $h+k+l$=odd and (b) 0*kl* reflections with l=even which are allowed in P4/ncc but not in I4, and (c) several 0*kl* reflections with k, l=odd which are allowed in I4 but not in P4/ncc. All these reflections were checked with an azimuth-scan which rotates the crystal around the scattering vector. With this scan only the type (c) reflections were rejected. Furthermore, all the reflections that were observed by the electron diffraction measurements[1] but not allowed in either of the two space groups were examined in the same way. Consequently, all the observed peaks were found to be false ones.

The structure parameters of Bi_2CuO_4 were refined with a Rietveld refinement program RIETAN.[9] We started the refinement with P4/ncc space group using structure parameters obtained by Boivin *et al.*[6] (cf. Table I) because reflections in the powder diffraction data cannot be completely indexed on the bases of I4 space group as indicated by the X-ray single-crystal measurements. A preliminary refinement showed that preferred orientation was negligible. In later refinement stages, anisotropic thermal parameters were assigned to all the sites. It should be pointed out here that anisotropic thermal parameters, U_{ij}, were erroneously refined in the recent work of Ong *et al.*[3] For example, only U_{11}, U_{22} and U_{33} were varied for the O site, which is the general equivalent position, in their Rietveld refinement. For the centrosymmetric setting of P4/ncc space group, U_{ij}'s must be refined in a

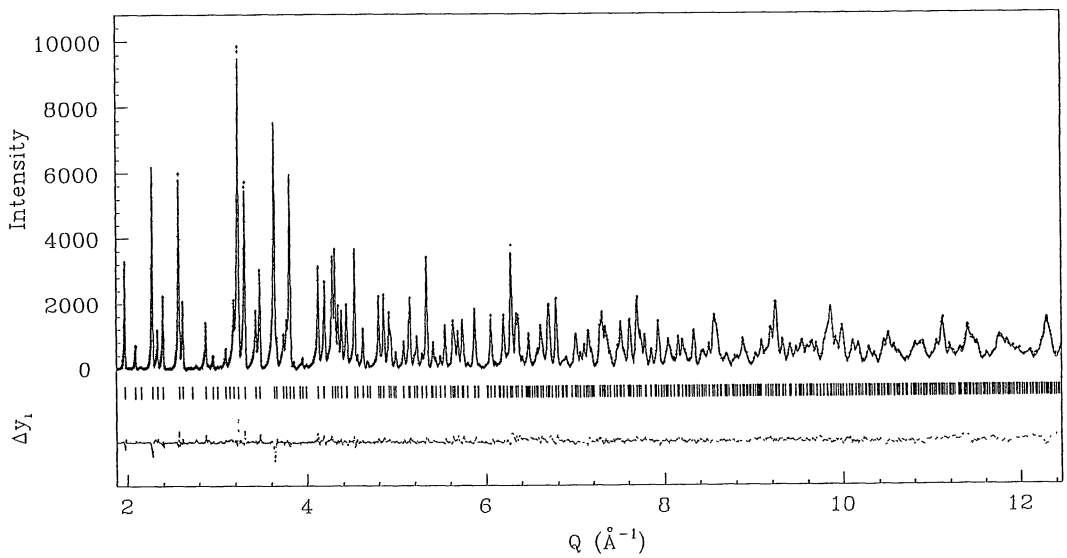

Fig. 2. Result of Rietveld refinement for Bi_2CuO_4. Background was fit as a part of the refinement but has been subtracted before plotting. Δy_i represents the difference between observed and the calculated intensities in the same scale.

Table I. Fractional coordinates and thermal parameters obtained by Rietveld refinement of neutron powder diffraction data for Bi_2CuO_4. Its space group is P4/ncc (No. 130, centrosymmetric setting). B_{eq} is the equivalent isotropic thermal parameter. Numbers in parentheses are statistical uncertainties of the last significant digit. Lattice constants are $a=8.5019(1)$ Å and $c=5.8196(1)$ Å. Final R factors are $R_{wp}=4.54\%$ ($R_e=3.01\%$), $R_p=3.43\%$, $R_B=3.12\%$ and $R_F=1.75\%$.

Atom	Site	x	y	z	U_{11}(Å^2)	U_{22}(Å^2)	U_{33}(Å^2)	U_{12}(Å^2)	U_{12}(Å^2)	U_{23}(Å^2)	B_{eq}(Å^2)
Bi	8f	0.58138(9)	$=1-x$	1/4	0.0043(3)	0.0054(12)	0.0105(5)	0.0007(5)	0	0	0.53
Cu	4c	1/4	1/4	0.9210(3)	0.0038(5)	$=U_{11}$	0.0128(10)	0	0	0	0.54
O	16g	0.45052(13)	0.35800(14)	0.9091(2)	0.0063(6)	0.0051(5)	0.0142(6)	−0.0009(5)	−0.0019(5)	0.0010(5)	0.67

Table II. Interatomic distances, l, in Bi_2CuO_4 at room temperature.

Bond	l (Å)	Multiplicity
Cu–O	1.9376(12)	4
Cu–Bi^{i}	3.3141(7)	4
Bi–O^{ii}	2.1302(14)	2
Bi–O^{iii}	2.7616(13)	2
Bi–O^{iv}	2.3321(14)	2
Cu–Cu^{i}	2.9098(0)	2
Bi–Bi^{ii}	3.506(1)	2

Symmetry codes: i) $1/2-x, y, 1/2+z$; ii) $1-x, 1-y, 1-z$; iii) $1/2+y, 1-x, 1-z$; iv) $x, y, -1+z$

manner described in Table I. Oxygen nonstoichiometry was further examined by refining the occupation factor, g, of the O site. The resulting g value was 0.995(4), which is virtually unity in view of the underestimation of standard deviations in Rietveld analysis. Thus, the g value of the O site was fixed at 1 in the final refinement.

Final R factors are $R_{wp}=4.54\%$ ($R_e=3.01\%$), $R_p=3.43\%$ and $R_B=3.12\%$. Figure 2 gives the observed (cross) and the calculated (solid line) intensities for the final fit and the differences (Δy_i) between them. This figure shows that the sample contains no appreciable amounts of impurities. Table I lists lattice constants, structure parameters and their standard deviations. Selected interatomic distances are given in Table II.

The interatomic distance between Cu and O is the shortest and is similar to that in 2D Cu-O sheets for high-T_c oxides. Therefore, the CuO_4 square plane is considered to form a tightly connected unit. A remarkable structural feature of this compound is that the CuO_4 square planes are not connected each other by sharing oxide ions in the plane as in the high-T_c oxides. Each CuO_4 square plane is connected via Bi ions. In Fig. 1 these second shortest Bi–O^{iv} bonds were drawn by dotted lines. It is clear from the figure that the CuO_4 square planes are connected along the [110] direction in a staggered manner. Since the interatomic distances along the [001] direction is much larger, the bonding along this direction is considered to be weaker. This interpretation is consistent with the fact that the single crystal can be easily cleaved with (001) as the

cleavage plane. The highly anisotropic thermal parameters listed in Table I also supports this picture; i.e., each atom in this structure has the largest component of thermal vibration along the [001] direction. Therefore, from the structural point of view, a 1D nature in magnetizm associated with of Cu^{2+} ions is difficult to be predicted.

3.2 *Magnetic structure*

As shown in Fig. 3 and Table III, several magnetic Bragg reflections which develop below 42 K are observed with neutron diffraction measurements. The magnetic intensity superposed on the nuclear reflection 00*l* (*l*=even) rejects the previously proposed structure model with the spin direction along the [001] axis.[2,3] It is noted that this type of magnetic reflections are observable only in the structure with staggered displacements of CuO_4 unit along the [001] axis which exist in the space group P4/ncc but not in I4. As shown in Table III, the observed intensities are consistent with a magnetic structure which is depicted in Fig. 1, where the moment is *not along the [001] axis but in the CuO_4 plane.* Due to both extinction effects and a lack of information about the anisotropic Q dependence of the magnetic form factor, refinement of the structure is difficult at this moment. Comparing the magnetic intensity with the nuclear one of 002, in which the extinction effect is small, we calculated the antiferromagnetic moment at 10 K to be $0.85 \pm 0.05\ \mu_B$. This value is larger than that obtained by the previous measurements because a wrong direction of the moment was assumed in them. According to a high field measurement below T_N,[10] the magnetization is linear to the field up to 26 T and the induced magnetization is only $0.2\ \mu_B$/Cu suggesting that the magnetic moments are tightly confined in the plane.

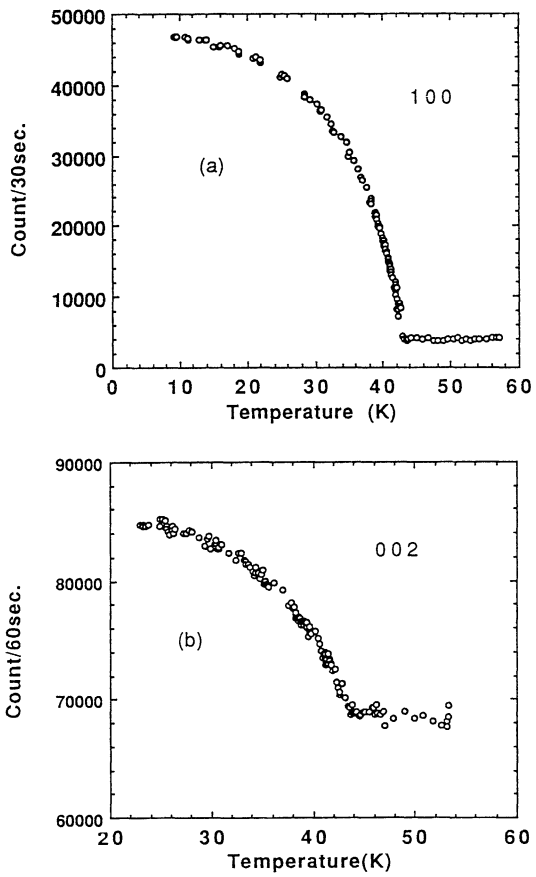

Fig. 3. Temperature variation of the Bragg reflections of (a) 100 and (b) 002. Note that in 002, magnetic intensity is superposed on the nuclear one.

Table III. Observed magnetic Bragg intensities vs calculated ones based on the structure model in Fig. 1.

Reflection	I_{obs}	I_{calc}
100	100(1)	100
300	13.8(2)	24
500	4.5(2)	5
302	15.4(10)	6
001	0.0(3)	0
002	65.5(12)	34
003	0.8(3)	0
004	25.4(4)	5

3.3 *Magnetic susceptibility and magnetization*

The temperature variations of the inverse magnetic susceptibilities for the single crystal of Bi_2CuO_4 are shown in Fig. 4. A magnetic field of 1.5 T was applied in both directions parallel and perpendicular to CuO_4 square planes. The previously reported broad peak around 50 K as well as the upturn below around 15 K are also observed in the present measurements. As shown in Fig. 5 however, below about 42 K, we found an unusual field

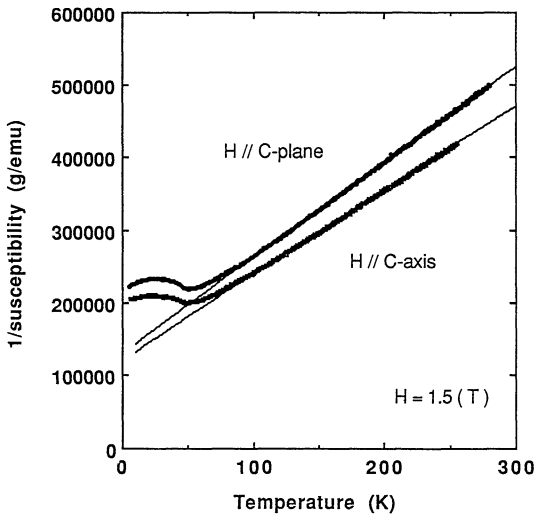

Fig. 4. Temperature variation of the inverse magnetic susceptibility of single-crystal of Bi_2CuO_4. External magnetic field of 1.5 T was applied parallel or perpendicular to the [001] direction. Solid lines are the calculation assuming the anisotropic g-values and Van Vleck paramagnetism.

dependence in the susceptibility with a magnetic field perpendicular to the [001] direction. The temperature dependence of the susceptibility around 42 K becomes steeper under a weaker field. This field dependent susceptibility is inconsistent with the anticipated 1D antiferromagnetism. Instead, as is observed in the neutron diffraction measurements, the temperature of 42 K corresponds to the Néel temperature for the 3D antiferromagnetic order, and the field dependent susceptibility is ascribed by a continuous rotation of the ordered moments as will be discussed later.

In Fig. 4, the background from sample cell and core diamagnetism were subtracted. Therefore, the anisotropy is attributed to the anisotropic Van Vleck paramagnetism and g-values of Cu spins. Then the temperature dependence of the susceptibilities between 150 K and 280 K was analyzed by the Curie-Weiss law with $S=1/2$ in addition to the anisotropic Van Vleck paramagnetism as,

$$\chi_{i(i=/\!/,\perp)}=N(g_i\mu_B)^2S(S+1)/\{3k_B(T-\theta_i)\}+\chi_i^{vv}, \quad (1)$$

where suffixes // and $\perp$ denote the directions of the applied magnetic fields parallel and perpendicular to the [001] direction, respectively. From the crystal field treatment the following formula can be applied for Cu^{2+} ($3d^9$) ions in square coordination of oxygen anions,

$$g_{/\!/}=2(1-4\lambda/E_{/\!/}),\quad g_\perp=2(1-\lambda/E_\perp), \quad (2)$$

$$\chi_{/\!/}^{vv}=8N\mu_B^2/E_{/\!/}\quad\text{and}\quad\chi_\perp^{vv}=2N\mu_B^2/E_\perp, \quad (3)$$

where λ is a spin-orbit coupling constant and E_i is an energy difference between the ground and the excited state through the coupling. Since both parameters of λ and E_i were sensitive to the temperature region for the fit, we failed to obtain the reliable values for λ and E_i. On the other hand, the g-values and paramagnetic Curie temperatures were uniquely determined as follows: $g_{/\!/}=2.16\pm0.04$, $g_\perp=2.07\pm0.04$ and $\theta=-96\pm2$ K for both field directions. An example of the fitted result is depicted by solid lines in Fig. 4. With this calculation the Van Vleck paramagnetism of 1.20×10^{-7} and 0.61×10^{-7} emu/g for $\chi_{/\!/}^{vv}$ and $\chi_\perp^{vv}$ are obtained, respectively. An ESR measurement on the single crystal gives $g_{/\!/}=2.21$ at room temperature[12] which is consistent with the present analysis.

The field dependent susceptibility in Fig. 5

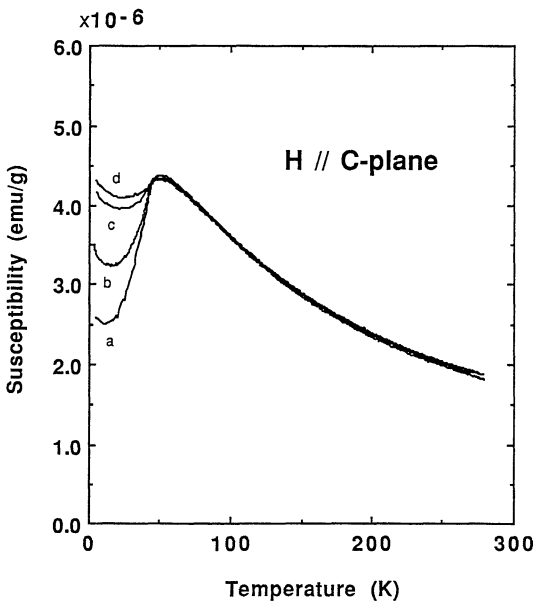

Fig. 5. Temperature variation of the magnetic susceptibility with magnetic fields of (a) 0.1 T, (b) 0.2 T, (c) 0.5 T and (d) 1.5 T applied perpendicular to the [001] direction.

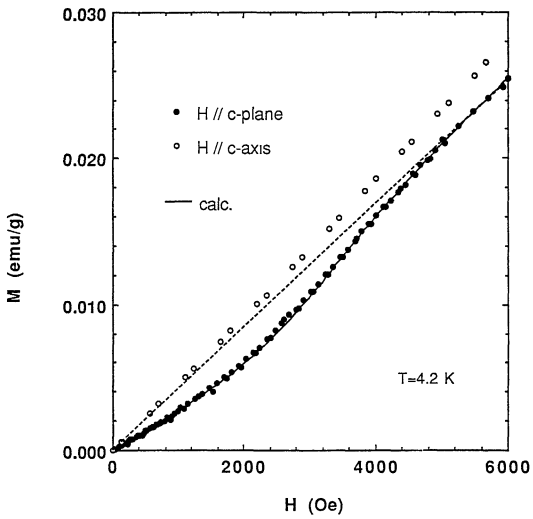

Fig. 6. Magnetization curves of single crystal Bi_2CuO_4 measured at 4.2 K. External magnetic field was applied parallel (open circle) or perpendicular (closed circle) to the [001] direction. Broken line is the extrapolated one from the higher field region up to 2 T. Solid line represents a calculation based on the model described in text.

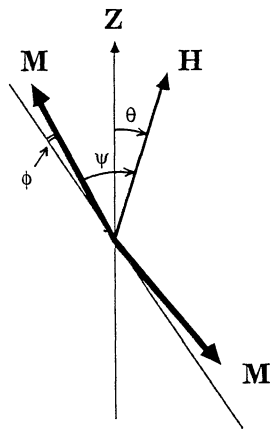

Fig. 7. Rotation of sublattice moments M under a magnetic field H. Z is the direction of the magnetic moment with $H=0$.

originates from a non-linear magnetization under a magnetic field perpendicular to the [001] axis as shown in Fig. 6. This non-linear magnetization was observed below T_N with a magnetic field between 0.05 and 0.5 T. Above 0.5 T and below about 0.05 T, the magnetization is linear to the field. On the other hand, non-linear magnetization is not observed for the field parallel to the [001] axis. This non-linear magnetization can be interpreted as spin rotations in the two antiferromagnetic domains. When a magnetic field is applied along the sublattice moments in one of the domain, a spin flop transition occurs at a critical field H_c resulting a jump in the magnetization. For another domain, since the sublattice moments are perpendicular to the field from the first, the magnetization is always linear to the field. A superposition of both magnetizations leads the non-linear magnetization similar to the experiment. Under a field in a general direction as shown in Fig. 7, sublattice moments continuously rotate from the initial magnetization axis and the jump in the magnetization is smeared out. The angle ψ between the moment and the external field is determined by a competition among exchange, anisotropy and Zeeman energies. If the exchange energy is much smaller than the others, one can neglect the angle ϕ which represents a tilt of the moment along the field. Then the ψ is determined by following equasions,

$$\tan 2\psi = \sin 2\theta / (\cos 2\theta - (H/H_c)^2), \quad (4)$$

and

$$H_c = (2K/(\chi_{perp} - \chi_{para}))^{1/2}. \quad (5)$$

Here, χ_{perp} and χ_{para} denote susceptibility for a field parallel and perpendicular to the sublattice moment, respectively and K is a constant of uniaxial anisotropy. Magnetization induced along the external field from both domains is written as,

$$M(H) = \chi_{perp} H(\sin^2\psi + \sin^2\psi') + \chi_{para} H(\cos^2\psi + \cos^2\psi'). \quad (6)$$

Here the angle ψ' represents an angle between H and the moment of the another domain. Initial susceptibility $M(H)/H$ corresponds to $(\chi_{perp} + \chi_{para})$ because $\psi' \approx \psi + 90°$ for small H. As the field increases, $M(H)/H$ asymptotically approaches to $2\chi_{perp}$ because both ψ' and ψ approach to 90°. As shown by a solid line in Fig. 5 the magnetization curve is almost perfectly reproduced by using the following parameters: $\theta = 25°$, $H_c = 0.34$ T, $\chi_{perp} = 2.13 \times 10^{-6}$ emu/g and $\chi_{para} = 0.27 \times 10^{-6}$ emu/g. From eq. (5) K was determined to be

10.7 erg/cc. It is noted that a unique magnetization axis in a domain was assumed in this model. Therefore a jump in the magnetization is expected under a field along one of the magnetization axis. Since the first measurement shown in Fig. 5 was done without adjusting the initial magmetization axis to the field direction, an additional magnetization measurement was carried out to search for the jump by rotating the crystal around the [001] axis. However, the magnetization showed only a continuous change for any direction of the magnetic field. The above mentioned analysis gave a minimum angle θ of 20°, which means that there exists an intrinsic angular distribution or dynamical fluctuation of the magnetic moment in this structure. We believe these results are not interpreted by finite temperature effect nor misalignment of the crystal.

One of the possible origin of the upturn of the susceptibility below about 15 K is free spins introduced by oxygen deficiencies and/or impurities. Assuming the spin value of 1/2, the number of such spin can be evaluated to be about 0.5% of O^{2-} ions which is within the detectable limit in the structural analysis. In order to examine the effect of the oxygen deficiencies the magnetic susceptibility measurement on the oxygen annealed powder sample was made but no remarkable difference between the annealed and the as-grown samples was found. Furthermore, below around 10 K the susceptibility starts to deviate from the $1/T$ law which suggests another mechanism for the upturn or additional phenomenon occurred by lowering the temperatures. An anomalous change in the ESR signal below around 10 K recently reported on powder sample[3] possibly is connected with the upturn and/or the fluctuation of the spin directions in the antiferromagnetic structure.

It is interesting to compare the magnetic properties of Bi_2CuO_4 with those of copper oxide with T'-structure because the nearest neighbor oxygen configuration around Cu ions is identical for these compounds. However the single crystals with T'-structure synthesized so far contain magnetic rare-earth ions which interact with Cu spins. $Sr_2CuCl_2O_2$ forms a tetragonal T-structure with apical chloride ions, then a similar nearest neighbor oxygen configuration around Cu ions to that of Bi_2CuO_4 is expected. In fact, this compound exhibits similar magnetic properties to Bi_2CuO_4, such as anisotropic susceptibility which can be described in the framework of crystalline field treatment, and non-linear field dependence of the magnetization under an in-plane magnetic field.[11] However, the temperature dependence of the susceptibility and the critical phenomena are quite different between the two: The susceptibility in $Sr_2CuCl_2O_2$ exhibits a weak temperature dependence typical to the 2D Heisenberg antiferromagnet with a large inplane exchange constant[11] in contrast to the Curie-Weiss behavior in Bi_2CuO_4. The temperature variation of the specific heat in the latter exhibits a well defined peak at T_N which is consistent with the development of the 3D magnetic order at T_N.[13] On the other hand, in the former no such peak has been observed due to the overwhelming 2D magnetic fluctuations at T_N. Since the Cu–O bond length is similar between the two, such a difference is attributed to the difference of the interaction path between Cu ions via oxygen ions.

In conclusion, the 3D and anisotropic antiferromagnetizm with $S=1/2$ of Cu^{2+} spins in Bi_2CuO_4 with the P4/ncc crystal symmetry is confirmed. Present study determines the 3D magnetic struture with a ferromagnetic stacking of Cu^{2+} spins along the [001] axis and with the spin direction in the CuO_4 plane. Neutron diffraction and scattering measurements are now continuing to elucidate the origin of the distribution or fluctuation of the moment below T_N and to study the short range spin correlations above T_N.

Acknowledgments

We are grateful to M. Motokawa and H. Nojiri for their measurements of ESR and high field magnetization on Bi_2CuO_4 and for invariable discussions. We would like to thank Y. Hidaka for his measurement of low field magnetization. We are also grateful to K. Kakurai for his neutron measurement to search for low dimensional spin correlations. The powder sample was synthesized with the

assistance of M. Onodera. This work was supported by a Grant-in-Aid for Science Research from the Ministry of Education, Science and Culture.

References

1) K. Sreedhar, P. Ganguly and S. Ramasesha: J. Phys. C **21** (1988) 1129.
2) J. P. Attfield: J. Phys. Condens. Matter **1** (1989) 7045.
3) E. W. Ong, G. H. Kwei, R. A. Robinson, B. L. Ramakrishna and R. B. Von Dreele: Phys. Rev. B **42** (1990) 4255.
4) S. Hosoya, T. Sumita, K. Yamada, K. Takada and Y. Endoh: to be published.
5) Z. V. Popovic, G. Kliche, M. Cardona and R. Liu: Phys. Rev. B **41** (1990) 3824.
6) J. C. Boivin, J. Trehoux and D. Thomas: Bull. Soc. Fr. Mineral. Crystallogr. **99** (1976) 193.
7) R. Arpe and Hk. Muller-Buschbaum: Z. Anorg. Allg. Chem. **426** (1976) 1.
8) B. K. Kakhan, V. B. Lazarev and I. S. Shaplygin: Zh. Neorg. Khim. **24** (1979) 1663.
9) F. Izumi, H. Asano, H. Murata and N. Watanabe: J. Appl. Crystallogr. **20** (1987) 3824.
10) H. Nojiri and M. Motokawa: private communication.
11) D. Vaknin, S. K. Sinha, C. Stassis, L. L. Miller and D. C. Johnston: Phys. Rev. B **41** (1990) 1926.
12) M. Motokawa: private communication.
13) N. Tomonaga, K. Takada and T. Suzuki: unpublished data.

Note added in proof—After the submission of this paper, we have found two independent neutron powder diffraction studies on Bi_2CuO_4 by J. García-Muñoz *et al.* published in J. Phys. Condens. Matter **2** (1990) 2205 and by J. Konstantinovic *et al.* published in J. Phys. Condens. Matter **3** (1991) 381. Both works have observed 3D magnetic order below T_N. However, since they observed no intensities in the magnetic (002), they assumed the moment direction along the [001] which is proved to be incorrect by the present study.